J. Fluid Mech. (1993), *vol.* 247, *pp.* 489–502

Stability of the interface in co-extrusion flow of two viscoelastic fluids through a pipe

By KANG PING CHEN AND YI ZHANG

Department of Mechanical and Aerospace Engineering, Arizona State University, Tempe, AZ 85287-6106, USA

(Received 19 April 1992 and in revised form 26 August 1992)

The linear stability of co-extrusion flow of two upper convected Maxwell fluids through a pipe at low Reynolds numbers is studied for arbitrary wavelength disturbances. The fluids interface can become unstable due to various mechanisms. It is shown that elasticity of the fluids can stabilize the capillary instability and a linearly stable interface can be achieved by appropriate choice of controlling parameters.

1. Introduction

Maintaining a stable interface between two viscoelastic fluids is of fundamental importance to co-extrusion, a method frequently used for forming composite materials of desired mechanical and optical properties. Various interfacial instabilities have been observed during co-extrusion and a thorough understanding of these interfacial instabilities is essential for this as well as many other industrial processes.

Interfacial instabilities usually occur in shear flows of multiple viscous and viscoelastic fluids. Using a linear stability analysis, Yih (1967) has shown that an interfacial instability can occur at vanishingly small Reynolds numbers for plane Couette/Poiseuille flow of two viscous Newtonian fluids and this instability is due to a stratification in fluid viscosities. There are many recent investigations on interfacial instabilities in various shear flows of viscous Newtonian fluids. The recent monograph of Joseph & Renardy (1992) gives the most comprehensive summary of these studies. However, very few investigations on interfacial instabilities of viscoelastic fluids in shear flows have been conducted (Larson 1992). One of the major conclusions drawn from the early studies concerning viscoelastic fluids is that the elasticity of the fluids can affect interfacial instabilities only when the viscosities of these two fluids are different. Thus, matching the viscosities of two fluids should eliminate interfacial instabilities. Viscosity matching has been used as a 'rule-of-thumb' in the polymer industry for a long time. However, it has been observed that interfacial instabilities can still occur even when the viscosities of the fluids are matched. This phenomenon was not explained theoretically until the recent works of Renardy (1988) and Chen (1991*a*, *b*). Chen (1991*b*) explicitly showed that an incorrect interfacial condition has been applied in all of the previous studies, except the most recent ones by Renardy (1988) and Chen (1991*a*), on interfacial instability problems of two viscoelastic fluids. With the corrected interfacial condition, a stratification in elasticity can induce an interfacial instability, even in the absence of density and viscosity stratifications.

For flow through a circular pipe, Chen (1991*a*) and Chen & Joseph (1992) have carried out linear analyses on the stability of the interface between two co-extruded

upper convected Maxwell (UCM) fluids to long-wave and short-wave disturbances, respectively. These studies indicate that in both long-wave and short-wave limits, the interfacial mode, and only the interfacial mode, can become unstable. Elasticity is shown to have a dominant effect on these interfacial instabilities when inertia is small. Thus the elastic property of the co-extruded fluids plays an important role in determining the stability of the interface, since inertia is usually very small for the co-extrusion process.

The stability diagrams for the long-wave and short-wave limits obtained by Chen (1991*a*) and Chen & Joseph (1992) indicate that the long- and short-wave interfacial instabilities in co-extrusion flow can be avoided by proper choices of controlling parameters. This suggests the possibility of maintaining a smooth fluids interface, linearly stable to infinitesimal disturbances of *all* wavelengths, for co-extrusion flow through a pipe. In this paper, we generalize the analyses of Chen (1991*a*) and Chen & Joseph (1992) to arbitrary wavelength disturbances. We demonstrate, through constructing stability diagrams in the Weissenberg number *vs.* wavenumber plane for various parameters, that it is indeed possible to find regions in controlling parameter space for which the interface is linearly stable. Stability diagrams corresponding to a given pair of viscoelastic fluids and die geometry can lead to the identification of appropriate operating conditions, and thus provide qualitative guidance for co-extrusion practice.

In §2, we formulate the general linearized equations at the fluid interface and discuss all the possible interfacial instabilities driven by various jumps across the interface. We then study a relatively simpler case in which both the core and the annulus fluids are modelled by the UCM constitutive equation. We show in §3 that elasticity of the fluids can stabilize the capillary instability and we present neutral stability diagrams for selected parameters in §4.

2. Origins of interfacial instabilities

Consider co-extrusion flow of two immiscible viscoelastic fluids through a circular pipe of inner radius R_2, driven by a constant pressure gradient $\partial\hat{P}/\partial x(<0)$, where the fluids are forced to flow in the positive x-direction. Fluid 1 is located in a core region (region 1) and fluid 2 in the annulus surrounding the core (region 2). The governing equations admit a unidirectional flow solution with a perfect cylindrical fluids interface $r = R_1$ when gravitational forces are negligible or when the pipe is arrange vertically. We are interested in the linear stability of this core–annular flow, for which the velocity in the core and the annulus are given by $\hat{\boldsymbol{U}}_i = \boldsymbol{e}_x \hat{W}_i(r)$, $i = 1, 2$. The non-zero extra stress components are $\hat{S}_{rx}(r)$, $\hat{S}_{rr}(r)$, $\hat{S}_{\theta\theta}(r)$, $\hat{S}_{xx}(r)$ in each region, where the stress tensor is $\hat{\boldsymbol{T}} = -\hat{P}\boldsymbol{I} + \hat{\boldsymbol{S}}$. The transverse pressure gradient is given by

$$\frac{\partial \hat{P}}{\partial r} = \frac{1}{r}\frac{\mathrm{d}(r\hat{S}_{rr})}{\mathrm{d}r} - \frac{\hat{S}_{\theta\theta}}{r} = \hat{S}'_{rr}(r) + \frac{\hat{N}_2}{r}, \tag{2.1}$$

where prime stands for the derivative with respect to the radial coordinate r, and the second normal stress difference $\hat{N}_2$ is defined as

$$\hat{N}_2 = \hat{S}_{rr}(r) - \hat{S}_{\theta\theta}(r). \tag{2.2}$$

We also define the first normal stress difference $\hat{N}_1$:

$$\hat{N}_1 = \hat{S}_{xx}(r) - \hat{S}_{rr}(r). \tag{2.3}$$

If the velocity, pressure and extra stress perturbations are $\boldsymbol{u} = \boldsymbol{e}_r u + \boldsymbol{e}_\theta v + \boldsymbol{e}_x w$, p and $\boldsymbol{S}$, and the fluids interface is perturbed to $R_1 + \delta(x, \theta, t)$, then the linearized equations for the disturbances at the unperturbed interface $\Sigma_0 : r - R_1 = 0$ are

$$u = \frac{\partial \delta}{\partial t} + \hat{W}(R_1)\frac{\partial \delta}{\partial x}, \tag{2.4}$$

$$[\![u]\!] = 0, \tag{2.5}$$

$$[\![v]\!] = 0, \tag{2.6}$$

$$[\![w]\!] + [\![\hat{W}'(R_1)]\!]\,\delta = 0, \tag{2.7}$$

$$[\![S_{rx}]\!] + [\![\hat{S}'_{rx}]\!]\,\delta - [\![\hat{N}_1]\!]\frac{\partial \delta}{\partial x} = 0, \tag{2.8}$$

$$R_1 [\![S_{r\theta}]\!] + [\![\hat{N}_2]\!]\frac{\partial \delta}{\partial \theta} = 0, \tag{2.9}$$

$$-[\![p]\!] + [\![S_{rr}]\!] - [\![\hat{N}_2]\!]\frac{\delta}{R_1} - \frac{\sigma}{R_1^2}\left(\delta + R_1^2\frac{\partial^2 \delta}{\partial x^2} + \frac{\partial^2 \delta}{\partial \theta^2}\right) = 0, \tag{2.10}$$

where σ is the interfacial tension coefficient and $[\![\ ]\!] = (\ )_1 - (\ )_2$ is the jump across the unperturbed interface $r = R_1$.

Bhatnagar & Giesekus (1970) have shown that Poiseuille flow of a single viscoelastic fluid in a circular pipe is stable to infinitesimal disturbances at low Reynolds numbers. When a straight streamline is perturbed to a curved shape, the tension along the straight streamline (first normal stress) created from the base Poiseuille flow will pull the streamline back to its straight position. In the presence of a fluids interface, however, an interfacial mode is introduced and this mode can become unstable due to a discontinuity across the interface in either perturbation velocity or perturbation stress.

All the possible causes of the interfacial instabilities can be identified from the set of interfacial equations, (2.4)–(2.10). The term $[\![\hat{W}'(R_1)]\!]\,\delta$ in (2.7) induces a discontinuity in the streamwise perturbation velocity w. This discontinuity of the streamwise perturbation velocity can cause an interfacial instability. Since the jump in the slope of the base flow velocity profile $[\![\hat{W}'(R_1)]\!]$ is proportional to the viscosity difference of these two fluids, this instability is due to a viscosity stratification. This type of interfacial instability was first discussed by Yih (1967) for planar geometry and has been the subject of many recent investigations for various shear flows of two immiscible Newtonian fluids (Hickox 1971; Hooper & Boyd 1983, 1987; Joseph, Renardy & Renardy 1984; Yiantsios & Higgins 1988; Preziosi, Chen & Joseph 1989; Hu & Joseph 1989; Chen, Bai & Joseph 1990; Chen & Joseph 1991). The conditions under which this instability occurs usually depend on the relative volume and the arrangement of the fluids.

Two terms can make the streamwise perturbation shear stress S_{rx} discontinuous across the interface: $[\![\hat{S}'_{rx}]\!]\,\delta$, and $[\![\hat{N}_1]\!]\,\partial\delta/\partial x$ (equation (2.8)). $[\![\hat{S}'_{rx}]\!]\,\delta$ is due to non-parabolicity of the base flow velocity profile and it vanishes for constant-viscosity fluids when gravitational force is negligible. An example for which this term is non-zero is that of vertical core–annular flow of two Newtonian fluids with different densities. In this case, $[\![\hat{S}'_{rx}]\!]$ is proportional to the density difference and it can

introduce an interfacial instability (Hickox 1971; Smith 1989; Chen *et al.* 1990). The second term $[\![\hat{N}_1]\!]\,\partial\delta/\partial x$ is present for viscoelastic fluids only, because $\hat{N}_1$ is the first normal stress difference of the base flow at the interface which is identically zero for Newtonian fluids. This term can drive an elastic interfacial instability in shear flows of multiple viscoelastic fluids even in the absence of viscosity and density stratifications, an instability first revealed by Renardy (1988) for planar geometry and later examined in detail by Chen (1991*a*, *b*) and Chen & Joseph (1992) for both planar and circular geometries. Hinch, Harris & Rallison (1992) have recently explored the physical mechanism for this elastic instability in the long-wave limit for co-extrusion flow in the case of matched viscosities and densities.

The circumferential perturbation shear stress $S_{r\theta}$ is not continuous for non-axisymmetric disturbances if the jump in the second normal stress difference of the base flow $\hat{N}_2 = \hat{S}_{rr}(r) - \hat{S}_{\theta\theta}(r)$ across the interface is not zero, as is evident from (2.9). A non-axisymmetric interfacial instability can thus result from this discontinuity. During the final preparation of this article, we become aware of the recent independent work of Hinch *et al.* (1992), the latest version of which includes a study of the effect of the jump in the second normal stress difference $[\![\hat{N}_2]\!]$ on the interfacial instability in the long-wave limit for the case of matched viscosities and densities, and zero interfacial tension. Their study for this special case shows that, indeed, the jump in $\hat{N}_2$ can drive a long-wavelength non-axisymmetric interfacial instability. They also find the conditions under which the growth rate of this non-axisymmetric mode dominates that of the axisymmetric mode caused by the jump in $\hat{N}_1$ for this special case. The second normal stress difference for most viscoelastic fluids is small, however, and we expect that the growth rate for the non-axisymmetric mode will be smaller than that for the axisymmetric mode in the presence of even a small amount of interfacial tension.

The jump in the second normal stress difference of the base flow can affect axisymmetric disturbances as well since it also appears in the normal-direction stress balance equation at the interface, (2.10). For axisymmetric disturbances, if we substitute the normal modes $f = \tilde{f}(r)\exp[i\alpha(x-ct)]$ into (2.10), where α is the streamwise wavenumber and c is the complex wave speed, we then obtain (after dropping the tilde)

$$-[\![p]\!] + [\![S_{rr}]\!] - \left\{\frac{[\![\hat{N}_2]\!]}{R_1} + \frac{\sigma}{R_1^2}(1-\alpha^2 R_1^2)\right\}\delta = 0. \tag{2.11}$$

In the long-wave limit for the case of matched viscosities and densities, the quasi-unidirectional approach of Hinch *et al.* (1992) can be applied and it can be easily verified from (2.11) that $[\![\hat{N}_2]\!]$ is destabilizing for long waves if $[\![\hat{N}_2]\!] > 0$, because it will then have the same sign as the interfacial tension term for $\alpha \to 0$. This implies that the effect of the jump in the second normal stress difference is destabilizing if the magnitude of the second normal stress difference of the core fluid is smaller than that of the annulus fluid, since $\hat{N}_2 < 0$ for most fluids. Hinch *et al.* (1992) have in fact obtained a formula for the growth rate for this long-wave instability for the case of matched viscosities and densities, and zero interfacial tension.

It is noted from (2.4)–(2.10) that when the interface is perturbed infinitesimally from its perfect cylindrical shape, various jumps in base flow properties will either drive the interface further away or push it back to its original location. Perturbation bulk motions are in general generated by these interfacial actions and they determine the stability of the interface. The way each driving mechanism enters into the determination of the stability is not obvious. This can be demonstrated by the

solution of the co-extrusion problem in the long-wave limit for UCM fluids (Chen 1991*a*). At the leading order in the long-wave limit the viscosity stratification (the $[\![\hat{W}'(R_1)]\!]\,\delta$ term in (2.7)) drives a neutrally stable secondary flow in the bulk. The elasticity of the fluids affects the interfacial stability not only through the jump in the first normal stress difference across the interface, $[\![\hat{N}_1]\!]$, but also through the elastic stresses associated with the leading-order secondary motion driven by the viscosity stratification. Even for zero stratification in the first normal stress difference, $[\![\hat{N}_1]\!] = 0$, the interface can become unstable due to the coupling of viscosity stratification and the elasticity of the fluids. An example of this case can be found from figure 5 of Chen (1991*a*) for UCM fluids. When $m_2 = 0.25$, $\beta = 4$, the jump $[\![\hat{N}_1]\!] = 0$, but instability occurs for $a = 2.5$ (see definitions for these parameters in (2.12) below).

The discussions above show that the fluids interface in co-extrusion flow can become unstable due to various mechanisms, some of which are reasonably understood and others that are yet to be thoroughly studied. How these driving mechanisms work in favour or against the stability of the interface could be subtle. In the remainder of this paper, we shall concentrate on the effect of the elasticity of the fluids on the stability and restrict our attention to the parameter ranges for which the interface is potentially stable. We employ a Chebyshev pseudo-spectral method (Canuto *et al.* 1988) to discretize the eigenvalue problem governing the linear stability to axisymmetric disturbances of co-extrusion flow of two UCM fluids with matched densities (equations (2.12)–(2.17) in Chen 1991*a*). The resulting generalized matrix eigenvalue problem is solved using the available IMSL routine EIGZC. Convergence tests have been conducted and the numerical results show good agreement with those of the asymptotic analysis. Care has been taken to detect spurious modes due to numerical discretization (Ho & Denn 1978; Lee & Finlayson 1986; Renardy & Renardy 1986; and Lim & Schowalter 1987). The following dimensionless parameters are used:

$$\left.\begin{aligned} a &= R_2/R_1, \\ (m_1, m_2) &= (1, \eta_2/\eta_1) \quad \text{(viscosity ratio)}, \\ \beta &= \lambda_1/\lambda_2 \quad \text{(relaxation time ratio)}, \\ Re_i &= \rho \hat{W}(0) R_1/\eta_i, \quad i = 1,2 \quad \text{(Reynolds numbers)}, \\ We_i &= \lambda_i \hat{W}(0)/R_1, \quad i = 1,2 \quad \text{(Weissenberg numbers)}, \\ Ca &= \lambda_1 \sigma/(\eta_1 R_1) \quad \text{(interfacial tension parameter)}, \end{aligned}\right\} \tag{2.12}$$

where $\hat{W}(0)$ is the centreline velocity of the basic flow, η is the viscosity and λ is the relaxation time in the UCM model. Note that $Re_1/Re_2 = m_2$, $We_1/We_2 = \beta$. We shall use the core Reynolds number as our reference Reynolds number, $Re = Re_1$, and the core Weissenberg number as our reference Weissenberg number, $We = We_1$.

3. Elastic stabilization of the capillary instability

Capillary breakup of a viscoelastic liquid filament into droplets is a subject of great interest. Most of studies on surface-tension-driven breakup follow the linear approach first used by Rayleigh (1879). Earlier investigations on linear stability concerning a completely relaxed viscoelastic filament conclude that a disturbance will grow more rapidly on a viscoelastic filament than on a Newtonian filament with

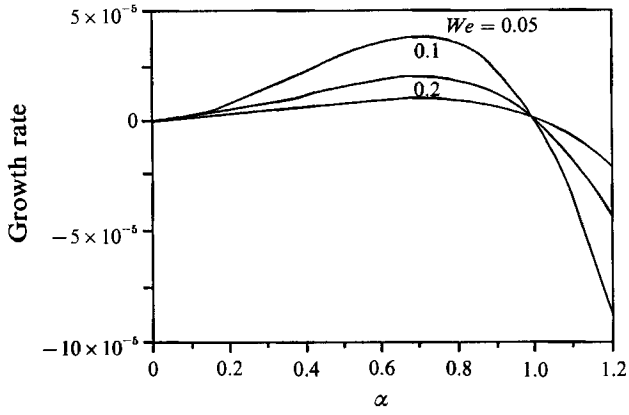

FIGURE 1. Growth rates for capillary instability on a sheared viscoelastic filament in an identical fluid medium. $a = 1.05$, $Ca = 0.2$, $Re = 0$. Weissenberg numbers are marked above each curve. Elasticity of the fluid is stabilizing.

the same shear viscosity. In fact, the linear stability problem for a viscoelastic filament reduces to that for a Newtonian filament with an effective viscosity. The elastic nature of the fluid is to make the effective viscosity smaller than the shear viscosity and thus increase the growth rate to a larger value (Goren & Gottlieb 1982). This result seems to disagree with experimental observations that it takes longer to break up a viscoelastic fluid filament by capillarity, which is believed to result from the large resistance of viscoelastic fluid to elongational stretching deformations. Goren & Gottlieb (1982) argue that un-relaxed tensile stress generated in the nozzle from which the jet is issued may explain the retarded breakup of a viscoelastic jet observed in the experiments. They add a constant residual tension to the linear analysis and find that this residual tension can stabilize the capillary instability from their approximate analysis. Bousfield *et al.* (1986), on the other hand, attribute the above discrepancy to the insufficiency of the linear stability analysis and performed a nonlinear study using a transient finite-element numerical method and an approximate one-dimensional analysis. Their results seem to agree well with available experiments.

Capillary breakup of a *sheared* viscoelastic filament in another viscoelastic or Newtonian medium has not been studied. The co-extrusion problem can serve as a model for such a study. The core fluid can break-up into slugs or drops due to the capillary instability, although the interfacial tension between polymeric fluids is usually small. For a Newtonian fluids system, Preziosi *et al.* (1989) have shown that the capillary instability, tending to break up a sheared Newtonian core filament, can be completely stabilized in some parameter range by sufficient shear of the fluids. Chen & Joseph (1991) further pointed out that this shear stabilization of capillary instability is due to the inertia of both the core and the annulus fluids. For viscoelastic fluids in co-extrusion flow, the Reynolds numbers of both the core and the annulus fluids are usually very small, either due to the large viscosity or the low velocity of the fluids. Thus, stabilization due to inertia is probably not enough to overcome the capillarity. However, high levels of elastic stress can provide another way to stabilize the capillary instability, which will be demonstrated by the following examples.

Figure 1 shows the growth rates of the capillary instability on a sheared viscoelastic filament in an identical fluid medium: $m_2 = \beta = 1$, for $a = 1.05$, $Ca = 0.2$,

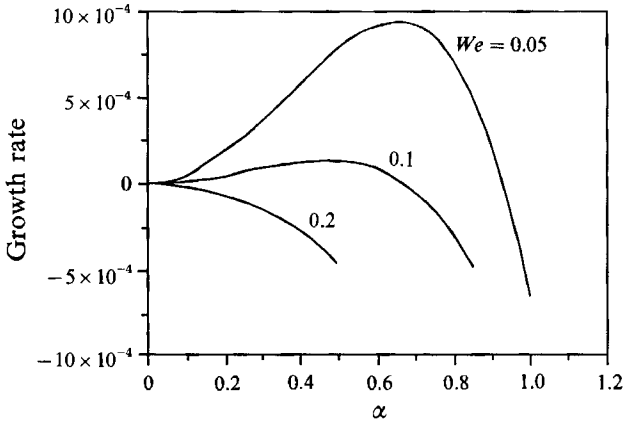

FIGURE 2. Growth rates for $a = 1.05$, $m_2 = 0.2$, $\beta = 1.6$, $Re = 0$, $Ca = 0.2$ and various Weissenberg numbers. Capillary instability is completely stabilized when $We = 0.2$.

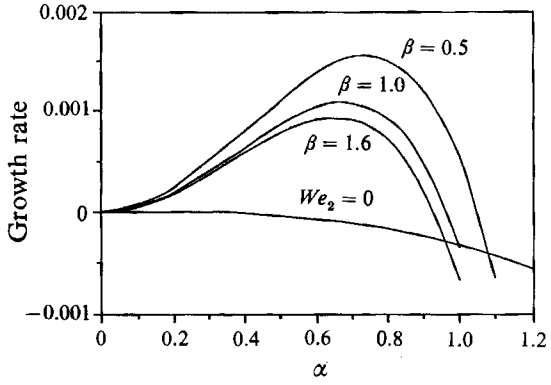

FIGURE 3. Effect of elastic stratification on capillary instability. $a = 1.05$, $m_2 = 0.2$, $Re = 0$, $Ca = 0.2$. A more elastic core, $\beta > 1$, is good for stabilization. $We_2 = 0$ corresponds to the case of a Newtonian annulus, for which the capillary instability is completely stabilized.

and zero inertia, $Re = 0$. The growth rate for large Weissenberg number is smaller than that for smaller Weissenberg number. This indicates that the tensile stress (first normal stress) developed along the streamlines for the sheared base flow is stabilizing the capillary instability. Moreover, the larger the normal stress, the stronger is this stabilization. The tension along the streamline retards even the linear growth of the capillary instability.

In figure 2 the growth rates for $a = 1.05$, $m_2 = 0.2$, $\beta = 1.6$, $Re = 0$, $Ca = 0.2$ are plotted for $We = 0.05, 0.1, 0.2$. This corresponds to a situation of fixed viscosity ratio and fixed elasticity ratio between the core and annulus fluids. The growth rate for the capillary instability is reduced tremendously by increasing the Weissenberg number. Increasing Weissenberg number can be thought of as either increasing the extrusion speed for given fluids or, for given extrusion speed, increasing the elasticity of both fluids while keeping their ratio fixed. When the elastic stress is large enough, $We = 0.2$, the capillary instability is completely stabilized.

Figure 3 shows how a stratification in elasticity affects the capillary instability. The growth rates plotted are for $a = 1.05$, $m_2 = 0.2$, $Re = 0$, $Ca = 0.2$, fixed Weissenberg number, $We = 0.05$ and various relaxation time ratios. The curve for

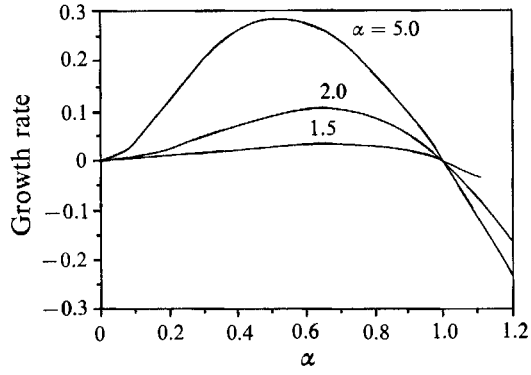

FIGURE 4. Growth rates for different sizes of core. $m_2 = 0.2$, $Re = 0$, $Ca = 0.2$, $\beta = 1.6$, $We = 0.05$. The larger the core, the stronger is the elastic stabilization.

$\beta = 1$ corresponds to the case of equal elasticity. The growth rate for a more elastic annulus, $\beta = 0.5$, is larger than that for equal elasticity, and the opposite is true for a less elastic annulus, $\beta = 1.6$. Thus a more elastic core is beneficial for stabilization of the capillarity. For the case of a Newtonian annulus, $We_2 = 0$, the capillary instability is completely stabilized.

The effect of the size of the core relative to the pipe on the capillary instability is shown in figure 4, for $m_2 = 0.2$, $Re = 0$, $Ca = 0.2$, $\beta = 1.6$, and $We = 0.05$. When a is small (corresponding to a situation in which the interface is close to the pipe wall), the shear rate in the core is large and so is the elastic stress. Thus the growth rates for small values of a are smaller than those for larger values due to the higher level of elastic stress, which is stabilizing.

The above examples illustrate that the elasticity of the fluids can be very effective in stabilizing the capillary instability. However, this stabilization does not work uniformly for all the combinations of parameters. In fact elastic destabilization could occur in some parameter range. It is a tremendous task to find the parameter ranges for which the elasticity of the fluids stabilizes the capillarity in low-speed flow, due to the large number of parameters present. Some suggestive information, however, can be obtained by inspecting figures 4 and 5 of Chen (1991*a*), which are the neutral stability curves in the long-wave limit $\alpha \to 0$. In general, for any fixed viscosity ratio m_2, the elasticity of the fluid is stabilizing if the volume of the more elastic component exceeds a critical volume which depends on the viscosity ratio m_2. For any fixed volume ratio we can also find ranges for the viscosity ratio m_2 and relaxation time ratio β for which the elastic effect is stabilizing. Most of the parameters used in the above examples fall in the regions where elasticity is stabilizing the longest waves, $\alpha \to 0$. The exceptions are those for $a = 2.0, 5.0$ in figure 4, for which elasticity destabilizes the longest waves.

4. Stability diagrams

The linear stability of the interface between two co-extruded UCM fluids is controlled by many parameters. In co-extrusion practice, however, we are interested in the parameters for which the interface is stable. Thus, stability diagrams in parameter space are of value since they can provide qualitative guidance for co-extrusion operation. In this section, we demonstrate, by constructing stability

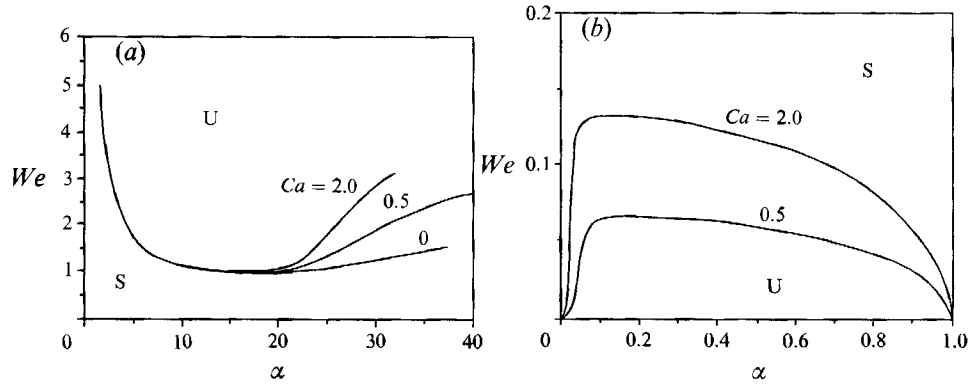

FIGURE 5. Neutral curves for $a = 1.05$, $m_2 = 0.2$, $\beta = 1.6$, $Re = 0$, and $Ca = 0$, 0.5, 2.0. There are two branches. Stable and unstable regions are marked by 'S' and 'U' respectively. (*a*) Upper branches; (*b*) lower branches.

diagrams in the (We, α)-plane for selected parameters, that a linearly stable fluids interface can indeed be maintained for an appropriate choice of parameters. These stability diagrams are by no means exhaustive, rather they serve as examples showing the existence of such stability regions in the parameter space.

We first study the case of $a = 1.05$, $m_2 = 0.2$, $\beta = 1.6$, and $Re = 0$. Figure 5 shows the neutral stability curves in the (We, α)-plane for various values of the interfacial tension parameter $Ca = 0$, 0.5, 2.0. There are two branches of the neutral curve: an upper branch and a lower branch. When the Weissenberg number We is small, the interface is unstable to the capillary instability whenever interfacial tension Ca is non-zero. When $Ca = 0$, the interface is stable at low Weissenberg numbers. The unstable region is larger for larger values of Ca, which represents stronger capillarity. This capillary instability can be stabilized by large elastic stress at higher values of the Weissenberg number. In fact, there exists a lower critical Weissenberg number beyond which the capillary instability is completely stabilized. For even higher values of Weissenberg numbers, an elastic instability can occur, as is evident in figure 5(*a*). This elastic instability occurs at relatively shorter wavelengths. The minimum of the upper neutral curve is very shallow so that for any supercritical Weissenberg number, waves of various wavelengths, ranging from 0.3 to 0.6 of the core radius ($10 \leqslant \alpha \leqslant 20$), are expected to be observed. The upper-branch neutral curve for $Ca = 0$ approaches the horizontal line $We = 3.8$ as $\alpha \to \infty$, as indicated by the asymptotic result for this case (Chen & Joseph 1992). Interfacial tension stabilizes the shortest waves, but the neutral curves for various values of Ca coincide with each other up to $\alpha = 20$. In particular, the upper critical Weissenberg number above which the elastic instability occurs remains almost the same for these different interfacial tensions, around unity.

The elastic effect is responsible for the high Weissenberg number instability shown in figure 5(*a*). For Newtonian fluids, viscosity stratification alone does not cause any interfacial instability when inertia is absent, because the eigenvalue c in this case is real and the perturbation flow driven by viscosity stratification is neutrally stable. For viscoelastic fluids, however, both the viscosity stratification and the jump in the first normal stress difference across the interface can drive a perturbation flow and the net perturbation flow is the superposition of these perturbation flows due to the linearity of the problem. Elastic effects are present in both these two perturbation

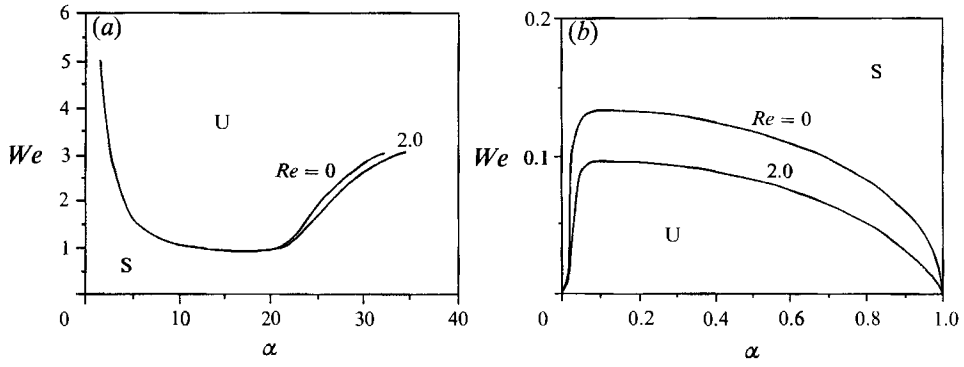

FIGURE 6. Inertia effect on interfacial stability. Neutral curves for $a = 1.05$, $m_2 = 0.2$, $\beta = 1.6$, $Ca = 2.0$ and $Re = 0, 2.0$. (a) Upper branches; (b) lower branches.

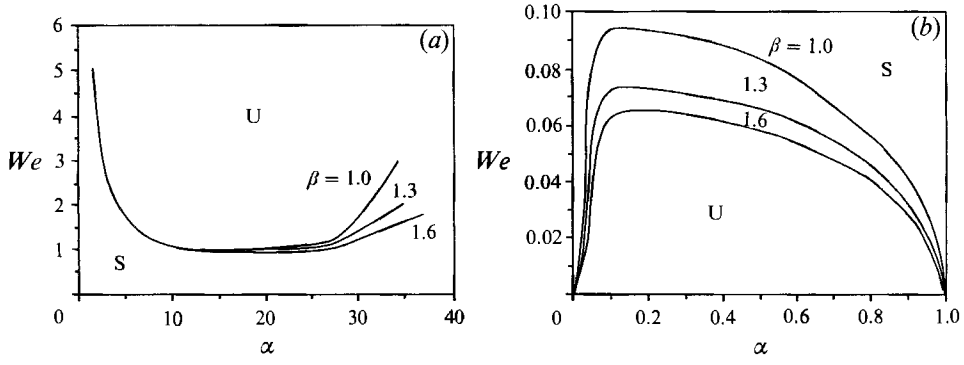

FIGURE 7. Effect of elasticity stratification on interfacial stability. Neutral curves for $a = 1.05$, $m_2 = 0.2$, $Re = 0$, $Ca = 0$ and various values of β. (a) Upper branches; (b) lower branches.

flows which together drives the instability at Weissenberg numbers higher than the upper critical value. When both the viscosity and the elasticity of the two fluids are the same, no instability other than the capillary one is found. This is consistent with the result of Bhatnagar & Giesekus (1970).

We next include the inertia effect. Figure 6 shows neutral curves for $a = 1.05$, $m_2 = 0.2, \beta = 1.6, Ca = 2.0$ and $Re = 0, 2.0$. Figure 6 (b) shows that the lower branch of the neutral curve for $Re = 2.0$ is lower than that for the inertia-less case of $Re = 0$, and thus inertia is stabilizing against the capillarity at low speed for these values of viscosity ratio and volume percentage. This stabilizing effect of inertia is also discussed by Chen & Joseph (1991) in the context of Newtonian fluids. For high Weissenberg numbers, on the other hand, inertia slightly lowers the upper branch for the portion of very short waves, $\alpha > 20$, but the upper critical Weissenberg number remains unchanged (figure 6a).

The effect of a stratification in relaxation time is demonstrated in figure 7 for $a = 1.05$, $m_2 = 0.2$, $Ca = 0.5$ and $Re = 0$. Figure 7 (b) shows that a more elastic core is beneficial for stabilizing the capillary instability. Increasing the elasticity of the core slightly lowers the short-wave portion of the upper branch of the neutral curve, as indicated by figure 7 (a).

Increasing the volume of the more elastic core fluid (decreasing a) has a stabilizing effect on the capillary instability (figure 8b), but a destabilizing effect on the elastic

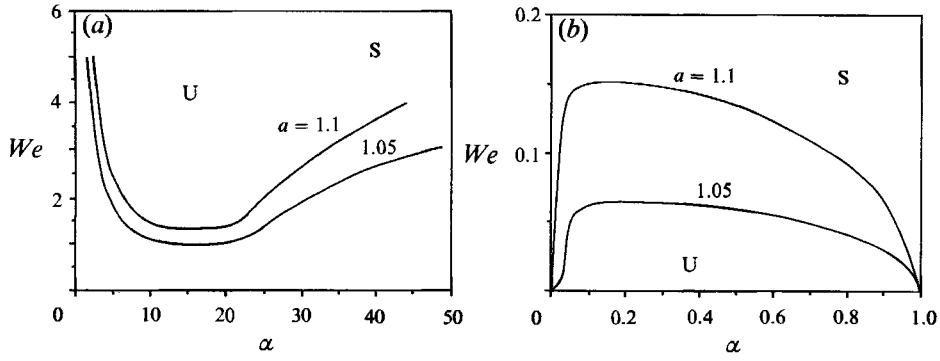

FIGURE 8. Neutral curves for $m_2 = 0.2$, $\beta = 1.6$, $Ca = 0.5$, $Re = 0$ and $a = 1.05$, 1.1. (a) Upper branches; (b) lower branches.

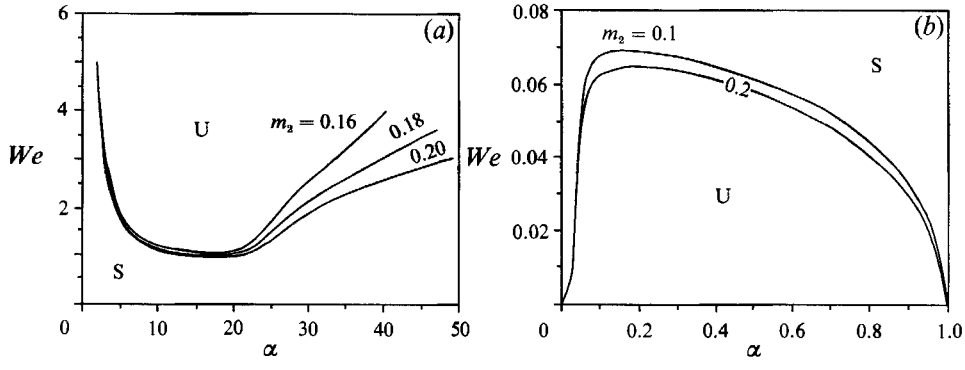

FIGURE 9. Neutral curves for $a = 1.05$, $\beta = 1.6$. $Ca = 0.5$, $Re = 0$ and various values of m_2. (a) Upper branches for $m_2 = 0.16$, 0.18, 0.20; (b) lower branches for $m_2 = 0.1$, 0.2.

instability (figure 8a). The shear rate at the interface is larger when the interface is closer to the pipe wall, i.e. when the parameter a is smaller. If the elastic effect is stabilizing the capillary instability, then increasing the volume of the core fluid (decreasing a) will intensify this stabilizing effect due to the increased shear rate and thus reduce the size of the unstable region of the capillary instability. On the other hand, this increased elastic stress lowers the upper branch because the upper branch instability is caused by the elastic effect associated with the perturbation flow driven by the viscosity stratification and elasticity stratification. Inspection of figure 8(a) indicates that, unlike other parameters, changing the volume of the core fluid, or equivalently changing the shear rate at the interface, changes the upper critical Weissenberg number considerably.

Viscosity ratio m_2 also alters the neutral stability curves. Figure 9(b) compares the lower branch of neutral curves for two viscosity ratios, $m_2 = 0.1$, 0.2, for the set of parameters $a = 1.05$, $\beta = 1.6$, $Ca = 0.5$ and $Re = 0$. Increasing the value for m_2 seems to have a stabilizing effect. Figure 9(a) compares the upper branch of the neutral curves for $m_2 = 0.1$, 0.18, 0.2, for the same set of parameters. In contrast to the lower branch, increasing m_2 has a destabilizing effect for the high Weissenberg number elastic instability. The shear rate in the core is proportional to m_2. Increasing m_2 will increase the normal stress in the core and thus has a stabilizing effect on the capillarity and a destabilizing effect on the elastic instability.

The neutral stability curves presented above demonstrate that it is possible to maintain a linearly stable smooth interface for co-extrusion flow. For the set of

parameters considered, we found that there are two critical Weissenberg numbers, a lower one and an upper one. The flow is unstable to the capillarity if the Weissenberg number is below the lower critical value and an elastic instability results if the Weissenberg number is larger than the upper critical value. For Weissenberg numbers between these two critical values, the flow is linearly stable to disturbances of arbitrary wavelength. The lower critical Weissenberg number is influenced by various parameters, but the upper critical Weissenberg number, about unity for the cases considered, seems to be insensitive to moderate changes in values of most of parameters, except that of volume ratio (or parameter a).

It should be emphasized, however, that various types of neutral curves are possible owing to the large number of parameters present. The effects of these parameters on the interfacial instability may vary, depending on the specific situations.

5. Conclusions

The stability of the fluids interface in pressure-driven co-extrusion flow of two viscoelastic fluids through a pipe is controlled by many parameters. Formulation of the linearized interfacial equations indicates that the fluids interface can become unstable to infinitesimal disturbances due to various mechanisms. For low Reynolds number flow, which is typical for co-extrusion process, interfacial tension and elasticity each can drive an interfacial instability. The most amplified waves for the high Weissenberg number elastic instability are relatively short. The elasticity of the fluids plays a dual role in determining the interfacial stability. It is shown that the capillary instability can be stabilized by increasing elastic stress and the elastic instability can be avoided by lowering elastic stress. It is possible to find regions in parameter space for which the interface is linearly stable. For the selected parameters used in this study, we have constructed neutral stability diagrams in the (We, α)-plane and we have found two critical Weissenberg numbers, $We_{c1} < We_{c2}$. The interface is linearly stable when the Weissenberg number takes values between these two critical numbers, $We_{c1} < We < We_{c2}$. These stability diagrams suggest that stability analysis can be used to provide qualitative guidance for co-extrusion practice.

The calculations presented in the present study are restricted to axisymmetric disturbances. For models which do not predict a second normal stress difference in viscometric flows, like the UCM used in this study, we expect that in the presence of interfacial tension, in general, the non-axisymmetric disturbances will be damped and the axisymmetric ones are the most dangerous.

It should be pointed out that the UCM constitutive equation used in calculating the stability characteristics in §§3 and 4 models real viscoelastic fluid only qualitatively and some of the important rheological behaviours, like shear thinning and second normal stress difference, are completely missed by this model. The emphasis of our present study is placed on the effect of streamwise elastic stress and should be regarded as only a first step towards the full understanding of the interfacial instabilities in co-extrusion flow. Hinch *et al.* (1992) study the second normal stress effect in an economical fashion for a special case. Further advances incorporating shear thinning and second normal stress difference effects require a more sophisticated rheological equation of state, and it is probably necessary to investigate both axisymmetric and non-axisymmetric disturbances. Nonlinear effects also need to be considered. The results obtained from such an analysis will be of great value for the relevant polymer industries.

This paper was first presented by K.C. at the 3M Technical Forum in November 1991 and we have benefited from discussions with 3M researchers. Thanks are due to D. D. Joseph for his continued interest and encouragement; to E. J. Hinch for supplying his paper in preprint form. The support of a PYI award from the National Science Foundation (CTS-9157063) is gratefully acknowledged.

REFERENCES

BHATNAGAR, R. K. & GIESEKUS, H. 1970 On the stability of viscoelastic flow. III. Flow in a cylindrical tube and an annulus. *Rheol. Acta* **9**, 412–418.

BOUSFIELD D.W., KEUNINGS, R., MARRUCCI, G. & DENN, M. M. 1986 Nonlinear analysis of the surface tension driven breakup of viscoelastic filaments. *J. Non-Newtonian Fluid Mech.* **21**, 79–97.

CANUTO, C., HUSSAINI, M. Y., QUARTERONI, A. & ZANG, T. A. 1988 *Spectral Methods in Fluid Dynamics*. Springer.

CHEN, K. 1991*a* Interfacial instability due to elastic stratification in concentric coextrusion of two viscoelastic fluids. *J. Non-Newtonian Fluid Mech.* **40**, 155–175.

CHEN, K. 1991*b* Elastic instability of the interface in Couette flow of viscoelastic liquids. *J. Non-Newtonian Fluid Mech.* **40**, 261–267.

CHEN, K., BAI, R. & JOSEPH, D. D. 1990 Lubricating pipelining. Part 3. Stability of core–annular flow in vertical pipes. *J. Fluid Mech.* **214**, 251–286.

CHEN, K. & JOSEPH, D. D. 1991 Long wave and lubrication theories for core–annular flow. *Phys. Fluids* A **3**, 2672–2679.

CHEN, K. & JOSEPH, D. D. 1992 Elastic short wave instability in extrusion flows of viscoelastic liquids. *J. Non-Newtonian Fluid Mech.* **42**, 189–211.

GOREN, S. L. & GOTTLIEB, M. 1982 Surface-tension-driven breakup of viscoelastic liquid threads. *J. Fluid Mech.* **120**, 245–266.

HICKOX, C. E. 1971 Instability due to viscosity and density stratification in axisymmetric pipe flow. *Phys. Fluids* **14**, 251–262.

HINCH, E. J., HARRIS, O. J. & RALLISON, J. M. 1992 The instability mechanism for two elastic liquids being co-extruded. *J. Non-Newtonian Fluid Mech.* **43**, 311–324.

HO, T. C. & DENN, M. M. 1978 Stability of plane Poiseuille flow of a highly elastic liquid. *J. Non-Newtonian Fluid Mech.* **3**, 179–195.

HOOPER, A. & BOYD, W. G. 1983 Shear flow instability at the interface between two viscous fluids. *J. Fluid Mech.* **128**, 507–528.

HOOPER, A. & BOYD, W. G. 1987 Shear flow instability due to a wall and a viscosity discontinuity at the interface. *J. Fluid Mech.* **179**, 201–225.

HU, H. & JOSEPH, D. D. 1989 Lubricated pipelining: stability of core–annular flow. Part 2. *J. Fluid Mech.* **205**, 359–396.

JOSEPH, D. D. & RENARDY, Y. 1992 *Fundamentals of Two-Fluids Dynamics*. Springer.

JOSEPH, D. D., RENARDY, Y. & RENARDY, M. 1984 Instability of the flow of immiscible liquids with different viscosities in a pipe. *J. Fluid Mech.* **141**, 319–345.

LARSON, R. G. 1992 Instabilities in viscoelastic flows. *Rheol. Acta* **31**, 213–263.

LEE, K. C. & FINLAYSON, B. A. 1986 Stability of plane Poiseuille and Couette flow of a Maxwell fluid. *J. Non-Newtonian Fluid Mech.* **21**, 65–78.

LIM, F. J. & SCHOWALTER, W. R. 1987 Pseudo-spectral analysis of the stability of pressure-driven flow of a Giesekus fluid between parallel planes. *J. Non-Newtonian Fluid Mech.* **26**, 135–142.

PREZIOSI, L., CHEN, K. & JOSEPH, D. D. 1989 Lubricated pipelining: stability of core–annular flow. *J. Fluid Mech.* **201**, 323–356.

RAYLEIGH, LORD 1879 On the instability of jets. *Proc. Lond. Math. Soc.* **10**, 4–13.

RENARDY, M. & RENARDY, Y. 1986 Linear stability of plane Couette flow of an upper convected Maxwell fluid. *J. Non-Newtonian Fluid Mech.* **22**, 23–33.

RENARDY, Y. 1988 Stability of the interface in two-layer Couette flow of upper convected Maxwell liquids. *J. Non-Newtonian Fluid Mech.* **28**, 99–115.

SMITH, M. 1989 The axisymmetric long-wave instability of a concentric two-phase pipe flow. *Phys. Fluids* A **1**, 494–506.

YIANTSIOS, S. G. & HIGGINS, B. G. 1988 Linear stability of plane Poiseuille flow of two superposed fluids. *Phys. Fluids.* **31**, 3225–3238.

YIH, C. S. 1967 Instability due to viscosity stratification. *J. Fluid Mech.* **27**, 337–352.